

Disturbing epithelial homeostasis in the metazoan *Hydra* leads to drastic changes in associated microbiota

Sebastian Fraune,^{1*} Yuichi Abe² and Thomas C. G. Bosch¹

¹Christian-Albrechts University Kiel, Zoological Institute, Olshausenstrasse 40, 24098 Kiel, Germany.

²Department of Biophysics, Graduate School of Science, Kyoto University, Kyoto 606–8502, Japan.

Summary

Microbes have profound influence on the biology of host tissue. Imbalances in host–microbe interaction underlie many human diseases. Little, however, is known about how epithelial homeostasis affects associated microbial community structure. In *Hydra*, the epithelium actively shapes its microbial community indicating distinct selective pressures imposed on the epithelium. Here, using a mutant strain of *Hydra magnipapillata* we eliminated all derivatives of the interstitial stem cell lineage while leaving both epithelial cell lineages intact. By bacterial 16S rRNA gene analysis we observed that removing gland cells and neurones from the epithelium causes significant changes in hydra's microbial community. Absence of interstitial stem cells and nematocytes had no effect on the microbiota. When compared with controls, animals lacking neurones and gland cells showed reduced abundance of β -Proteobacteria accompanied by a significantly increased abundance of a *Bacteroidetes* bacterium. This previously unrecognized link between cellular tissue composition and microbiota may be applicable to understanding mechanisms controlling host–microbe interaction in other epithelial systems.

Introduction

Epithelia of all animals are colonized by complex communities of microbes (Dale and Moran, 2006). Microbial perturbations and imbalances underlie many human diseases, but the complexity of most natural microbe–epithelial systems has precluded detailed studies of this

usually beneficial relationship. Recent studies suggest that reduced bacterial diversity in the colonic mucosa is involved in inflammatory bowel disease (Ott *et al.*, 2004; Frank *et al.*, 2007) and that commensal bacteria play a role in directing the development of the mammalian immune system (Mazmanian *et al.*, 2005). But despite the realization that constant recognition of the commensal microbiota by Toll-like-receptors plays a protective role in intestinal homeostasis (Rakoff-Nahoum *et al.*, 2004) and that a single microbial molecule, polysaccharide A, is implicated in protection from intestinal inflammatory disease (Mazmanian *et al.*, 2008), we know little about the mechanisms and dynamics of these complex interactions. Moreover, it remains uncertain to what extent epithelial homeostasis has influence over the associated microbial community structures.

Pioneering work by Rahat and Dimentman (1982) first demonstrated that bacteria also affect growth and development in the simplest animal at the tissue grade of organization, the early branched metazoan *Hydra*, which in the absence of bacteria has a drastically reduced budding rate. Previously, we analysed the microbiota in different species of *Hydra* and observed, unexpectedly, that each host species supports association with a different set of bacterial phylotypes (Fraune and Bosch, 2007). These observations indicated that *Hydra* epithelia play an active role in selecting their microbiota. The findings suggest strong selective constraints operating to shape the microbial community.

Compared with various mammalian epithelia, the hydra body plan represents a simplified version: It consists of only two cell layers with a limited number of cell types. All cell types in *Hydra* are derived from only three distinct stem cell lineages, the ectodermal and endodermal epithelial stem cells and the interstitial stem cell lineage (Bosch, 2008). Interstitial stem cells are multipotent cells located along the body column and can differentiate in a position-dependent manner into nematocytes, nerve cells, gland cells and gametes (Bosch, 2007). Given this morphological simplicity and the fact that there is no physical barrier between the epithelium and the microbes, we hypothesized that *Hydra* could also be used to uncover epithelial influences on microbial community structures *in vivo*. Exploring this mutual relationship is a

Received 3 September, 2008; accepted 4 May, 2009. *For correspondence. E-mail sfraune@zoologie.uni-kiel.de; Tel. (+49) 431 880 4149; Fax (+49) 431 880 4747.

critical step towards understanding how host and microbe communities remain in a mutual balance after long-term co-evolution.

Results

Epithelial homeostasis can be disturbed experimentally in Hydra magnipapillata strain sf1

To decipher putative links between epithelial homeostasis and species-level bacterial phylotypes, we made use of mutant strain sf1 of *Hydra magnipapillata* which has temperature-sensitive interstitial stem cells (Sugiyama and Fujisawa, 1978). Interstitial stem cells are located between the ectodermal epithelial cells and differentiate into both germline and somatic components such as

nerve cells, gland cells and nematocytes (Bosch, 2008). Treatment for a few hours at the restrictive temperature (28°C) induces loss of the entire interstitial cell lineage from the ectodermal epithelium while leaving both the ectodermal and the endodermal epithelial cells undisturbed (Terada *et al.*, 1988). Following temperature treatment, the animals were cultured at the permissive temperature (18°C) for up to 49 days (Fig. 1A). As shown in Fig. 1B–F, overall morphology and integrity of the animal body remains unaffected by the temperature treatment. Analysis of the cellular composition (Fig. 1G) clearly indicates the gradual disappearance of the entire interstitial cell lineage including interstitial stem cells, nematocytes, neurones and gland cells. Approximately 30–40 days after temperature treatment, the tissue nearly

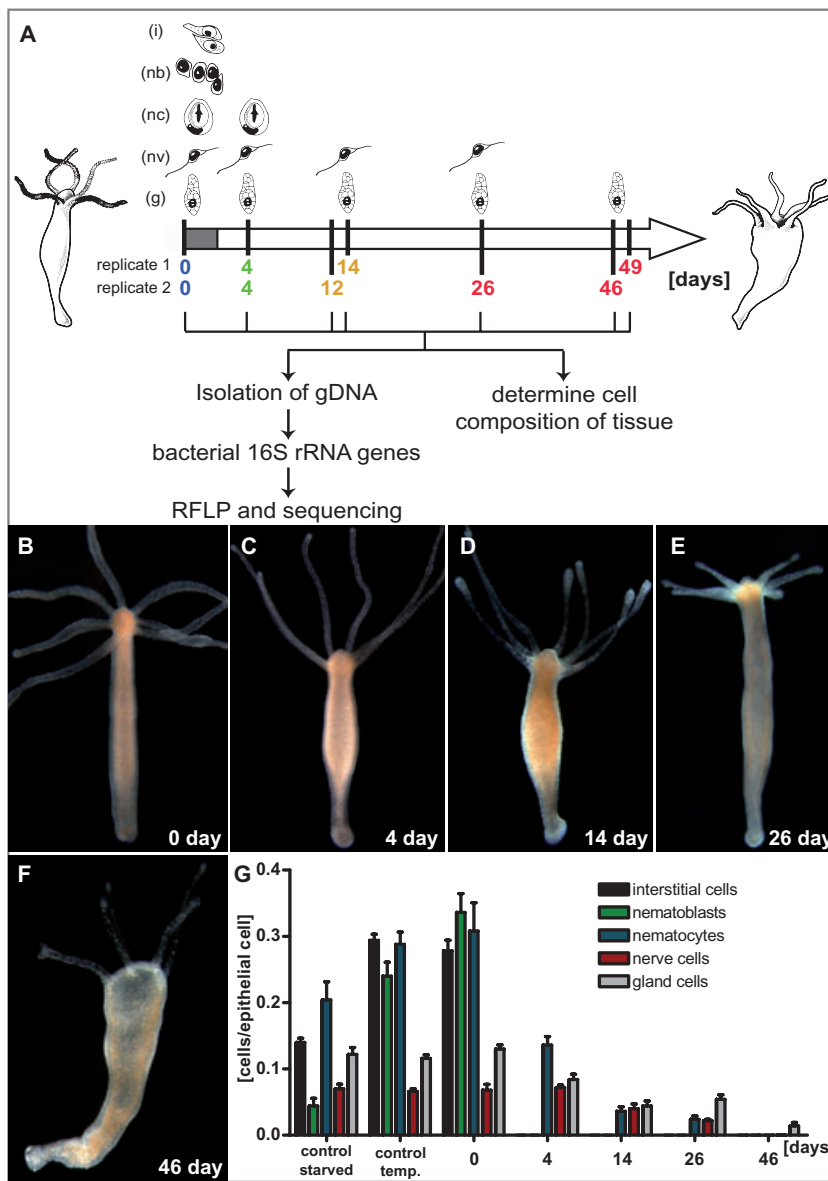


Fig. 1. Gradual disappearance of interstitial cell derivatives due to temperature treatment. **A.** Experimental design. Animals were cultured at non-permissive temperature for 2 days prior to culturing them at 18°C. From two independent replicates polyps were collected at various time points to determine the microbiota and to monitor changes in tissue composition. Cartoons illustrate the gradual disappearance of cell types from host tissue; (i) interstitial cells; (nb) nematoblasts; (nc) nematocytes; (nv) nerve cells; (g) gland cells. **B–F.** Live images of *Hydra magnipapillata* sf1 mutant at various time points after temperature treatment. As described (Sugiyama and Fujisawa, 1978), the epithelium is not affected by the temperature treatment. **G.** Cellular composition of polyps at different time points after temperature treatment. Note the absence of nearly all cells of the interstitial cell lineage 26–46 days after temperature treatment began. Control_starved, cellular composition of animals kept at 18°C but starved for 40 days. Control_temp., cellular composition of *Hydra magnipapillata* strain 105 46 days after temperature treatment. Note that in controls no change in nerve/epithelial and gland cell/epithelial cell ratios occur.

exclusively consists of endodermal and ectodermal epithelial cells. As treated polyps are unable to feed, for control we used animals starved for up to 40 days to exclude that changes in microbiota are due to changes in metabolic activity ('control_starved' in Fig. 1G). Comparing the cell composition in experimental animals at day 0 with control animals shows that in 'control starved' animals due to nutrient deprivation the number of fast proliferating cells such as interstitial cells and nematoblasts is reduced when compared with animals of day 0 (Fig. 1G) which were taken directly out from a well fed mass culture. Importantly, Fig. 1G shows that at day 0 the number of nerve cells and gland cells is about the same in controls and experimental animals. An additional control was performed to exclude that observed changes in bacterial composition are late responses to heat treatment. In a 'control_temp' experiment (Fig. 1G) we heat-treated the non-temperature-sensitive *H. magnipapillata* strain 105 and monitored the bacterial composition 46 days later.

Phylogenetic analysis reveals drastic differences in microbiota in control and disturbed epithelia

Next, we identified the microbiota in the hydra epithelium by performing a comprehensive bacterial 16S rRNA gene analysis at different time points after temperature treatment. The experiment was repeated two times independently with the sampling time points 0, 4, 14 and 49 days after temperature treatment in the first replicate and with the sampling time points 0, 4, 12, 26, 46 days after temperature treatment in the second replicate (Fig. 1A). For bacterial genotyping, genomic DNA was extracted from 10 animals from each sample and 16S rRNA genes were amplified by PCR and cloned. From each sample between 37 and 47 clones (Table 1) were randomly selected for restriction fragment length polymorphism

Table 1. Bacterial species richness in *Hydra magnipapillata* s1 mutant.

Sample	N	S	Chao 1	
			Mean \pm SD	95% CI
0-1	42	8	10 \pm 3	(8-23)
0-2	40	5	8 \pm 4	(5-30)
4-1	42	6	6 \pm 1	(6-7)
4-2	40	3	3 \pm 1	(3-4)
12-2	37	4	4 \pm 1	(4-5)
14-1	47	8	8 \pm 1	(8-14)
26-2	40	6	12 \pm 7	(7-43)
46-2	44	7	7 \pm 1	(7-13)
49-1	41	9	24 \pm 13	(12-77)
control_temp.	44	2	2 \pm 0	(2-2)
control_starved	40	3	3 \pm 1	(3-4)

N, total number of analysed clones; S, identified bacterial phylotypes; Chao1, richness estimator; CI, confidence interval.

(RFLP). To identify the bacterial species in the epithelium, partial sequences (~1450 bp) were obtained from each RFLP type. Following the phylogenetic analyses, sequences with $\geq 99\%$ similarity were designated as a phylotype. To characterize the bacterial community, we analysed the microbiota based on nearest relative (as determined by BLASTN search) and phylogenetic affiliation. Figure 2 shows the phylogenetic tree with 61 16S rRNA gene sequences representing 27 different phylotypes identified in the whole sequence data set. We uncovered two to three phylotypes in control tissue and three to nine phylotypes in the samples from the temperature-treated animals (Table 1). Analysis according to rarefaction curve (Fig. S1A and B) and non-parametric Chao1 algorithm (Table 1, Fig. S1C and D) indicate that most samples (except for 49-1, 26-2, 0-2) shown are comprehensive. The 16S rRNA sequences showed (Fig. 2) that bacteria of only a limited number of groups (predominantly β -Proteobacteria) are present in the two *H. magnipapillata* controls examined indicating strong selection. As *H. magnipapillata* is closely related to *H. vulgaris* (Hemrich *et al.*, 2007), most bacterial divisions present in the *H. magnipapillata* tissue had been documented earlier (Fraune and Bosch, 2007) when we examined the microbes in *H. vulgaris* tissue.

By identifying the bacteria species at distinct time points after temperature treatment, we next analysed whether and how perturbations in epithelial homeostasis contribute to changes in hydra's microbial community. Especially two bacterial phylotypes, belonging to the β -Proteobacteria and the *Bacteroidetes* (Fig. 2, grey shadowed phylotypes), could be identified at all sampling time points after temperature treatment. As shown in Fig. 3A and B, bacteria of the *Bacteroidetes* phylotype showed a 10–20-fold increase in relative abundance with increase from 7% to 69% in replicate 1 (Fig. 3A) and from 3% to 64% in replicate 2 (Fig. 3B). This increase in the abundance of *Bacteroidetes* is accompanied by decreased abundance of a bacteria of the β -Proteobacteria closely related to *Rhodospirillum rubrum*. Decrease in relative abundance was from 48% to 4% in replicate 1 (Fig. 3A) and from 83% to 14% in replicate 2 (Fig. 3B). To obtain additional support for the view that distinct bacterial phylotypes change in abundance with time after temperature treatment, we performed quantitative real-time PCR using phylotype-specific primers shown in Table 2. Figure 3C and D indicate that the overall abundance of bacteria was slightly reduced in all samples taken 2–4 weeks after temperature treatment. As 'control starved' animals show also a slightly reduced bacterial load, this most likely is due to nutrient deprivation. The data in Fig. 3C and D also reveal a decrease of abundance of the *Rhodospirillum* phylotype with the decrease being larger than the overall decrease of bacterial abundance. Intriguingly, about 2 weeks after temperature treatment we

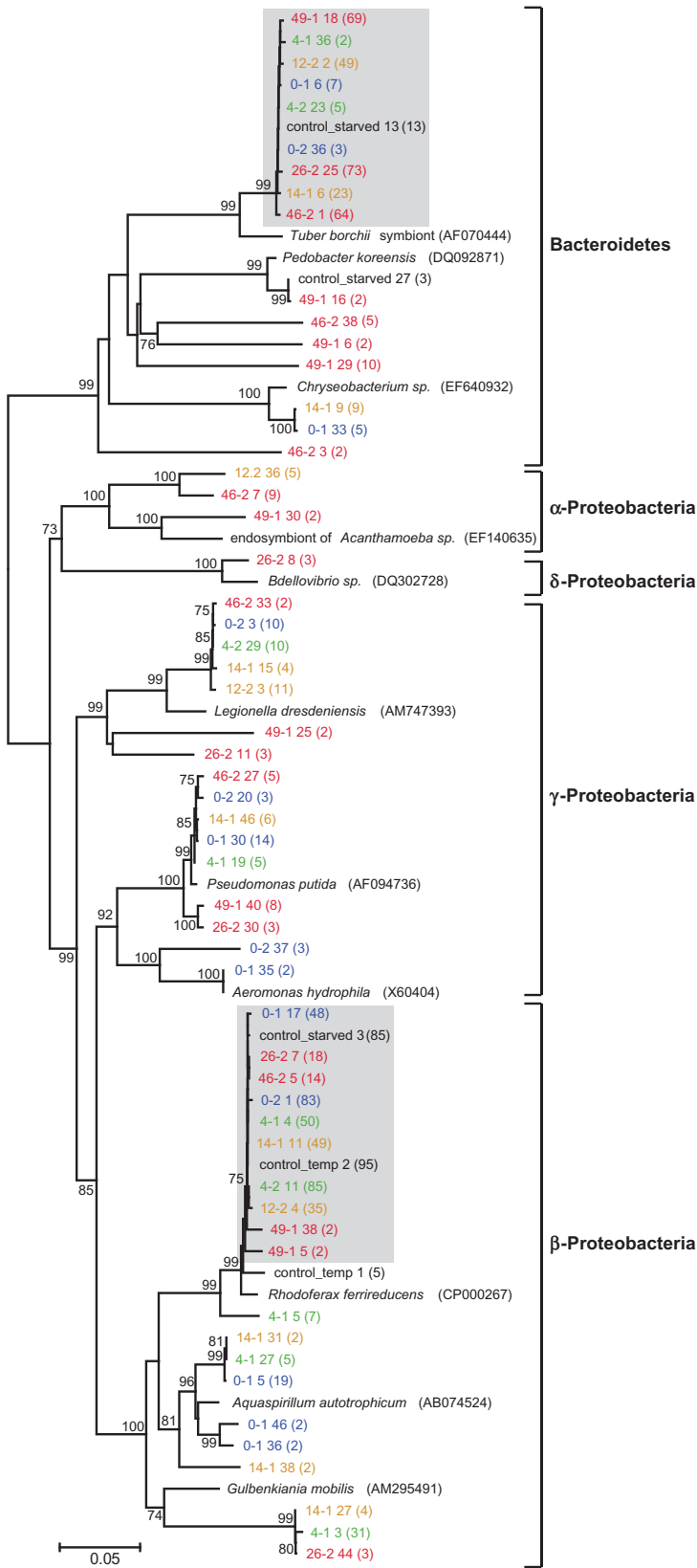


Fig. 2. Phylogenetic positions (16S rRNA gene sequences, neighbour-joining tree) of identified bacterial phylotypes. Bootstrap values are shown at the corresponding nodes ($n = 1000$), only bootstrap values ≥ 70 are indicated. Colour of phylotypes indicates different sampling time points; blue – 0 day, green – 4 days, yellow – 12, 14 days, red – 26, 46, 49 days after temperature treatment began. Phylotypes are encoded as followed 49-1 18 (69) = 49 days after temperature treatment, replicate one, clone 18, relative abundance of this phylotype 69% in the according sample. The branch length indicator displays 0.05 substitutions per site. Light grey shadowed sequences indicate two bacterial phylotypes showing changes in their relative abundance due to the temperature treatment.

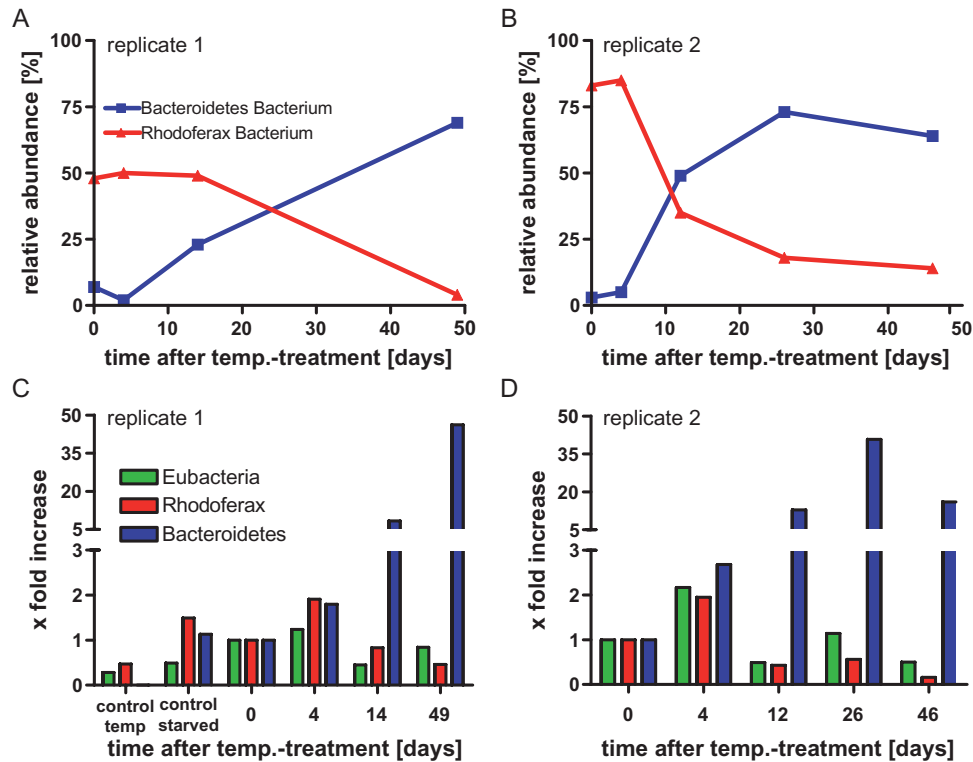


Fig. 3. Disturbance in tissue homeostasis leads to drastic changes in specific phylotypes of the colonizing microbiota. A and B. Relative abundance of bacterial phylotypes. C and D. Quantitative real-time PCR with phylotype-specific primers. Note that compared with two control and experimental animals at day 0 there are drastic changes in abundance of *Bacteroidetes* and *Rhodoferax* phylotypes while the overall bacterial load did only change slightly.

observed in both replicates a drastic increase of the *Bacteroidetes* phylotype (Fig. 3C and D).

To summarize these changes, we analysed the data by using the UniFrac computational tool (Lozupone and Knight, 2005) as described previously (Fraune and Bosch, 2007). UniFrac cluster analysis allowed assignment of distinct phylotypes to each tissue sample. As shown in Fig. 4, the bacterial composition of tissue samples from control and early time points after temperature treatment was very similar. In control tissue (both 'control starved' as well as 'control temp') as in tissue from polyps analysed before and immediately after tem-

perature treatment, bacteria belonging to the *Rhodoferax* phylotype are most abundant while bacteria of the *Bacteroidetes* phylotype were found only at very low relative abundance. As interstitial stem cells and early stages of nematocyte differentiation are eliminated within 2–4 days after temperature treatment (Fig. 1G), these cell types apparently had no immediate influence on microbial community composition. Intriguingly, 2 weeks after temperature treatment, when the host tissue was lacking not only all interstitial cells but also the nematoblasts and most nematocytes, and in addition also had a reduced number of neurones and gland cells (see Fig. 1G), the

Table 2. RT-PCR primers used in this study.

Name	Sequence (5'→3')	Position (bp) ^a	Target group	Perfect matches ^b		Reference
				Target group	Non-target group	
Bac1012_F	GAAAGGGATCTTCCAGCAATGG	1012–1033	<i>Bacteroidetes</i>	8 (0.01%)	0 (0.0%)	This study
Bac1134_R	CTCGCTGGTAACTAACAATAGG	1134–1113	<i>Bacteroidetes</i>	14 (0.02%)	2 (<0.001%)	This study
Rho1026_F	TCGAAAGAGAACCCTAACACAG	1026–1047	<i>Burkholderiales</i>	2 047 (5.6%)	97 (0.01%)	This study
Rho1148_R	AGAGTGCCCAACTAAATGTAGC	1148–1126	<i>Burkholderiales</i>	1 706 (4.6%)	239 (0.03%)	This study
Eub341F	CCTACGGGAGGCAGCAG	341–357	<i>Bacteria</i>	561 507 (70.7%)	14 (0.03%)	Muyzer <i>et al.</i> (1993)
Eub534R	ATTACGCGGCTGCTGGC	534–517	<i>Bacteria</i>	543 693 (68.5%)	282 (0.6%)	Muyzer <i>et al.</i> (1993)

a. Corresponding to the relative position in the *E. coli* 16S rRNA gene.

b. Determine by using the RDP database (Cole *et al.*, 2007).

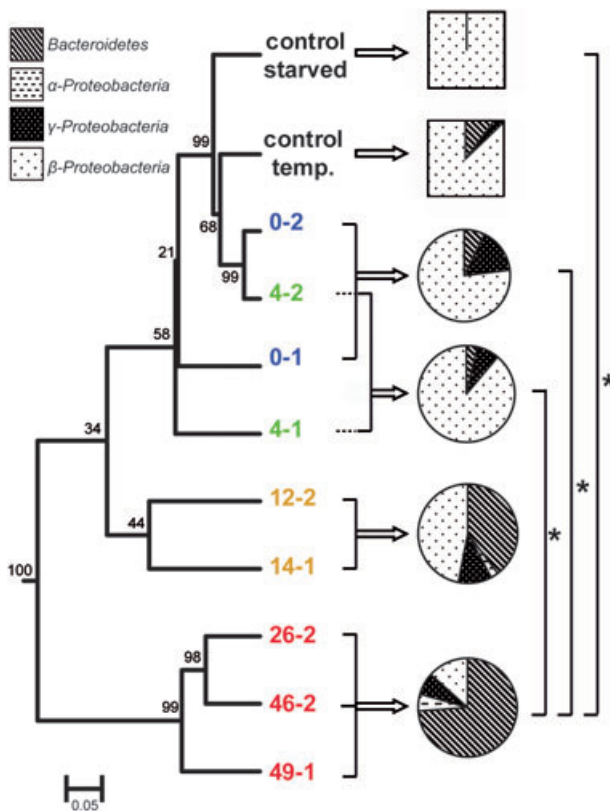


Fig. 4. Bacterial communities change when host tissue composition changes. Jackknife environment cluster tree (weighted UniFrac metric, based on the 61 sequence tree) of the analysed bacterial communities. 1000 Jackknife replicates were calculated, nodes are marked with Jackknife fractions. The branch length indicator displays distance between environments in UniFrac units. Coloured numbers indicate different sampling time points (for colour code see Fig. 2). Pie charts indicate relative abundance of bacterial phyla in different samples after temperature treatment. Data from similar sampling time points of the two independent replicates were pooled. Asterisks indicate the significance of the differences in the bacterial composition (UniFrac significance $P \leq 0.05$) of the pooled data sets.

bacterial composition changed. Most drastic changes in microbiota could be observed in polyps after about 4 weeks of temperature treatment compared with 0 day ($P = 0.04$, UniFrac significance). In these polyps nearly all of the cells of the interstitial cell lineage including nematocytes, nerve cells and gland cells had disappeared. As shown in Fig. 4, in samples from this disturbed epithelium the relative abundances of the *Rhodospirillum rubrum* and *Bacteroidetes* phylotype changed drastically. Taken together, our observations strongly indicate that the composition of the colonizing microbiota is dependent on host factors such as the cell types present in the epithelium.

Discussion

The data presented in this study show that changes in epithelial homeostasis in *Hydra* cause significant changes

in the microbial community, implying direct interaction between epithelia and microbiota. Which factors are involved in this dynamic interplay between host and microbes? As *Hydra* has complex epithelial cell-based mechanisms for host defence engaging novel potent antimicrobial peptides (Augustin *et al.*, 2009; Bosch *et al.*, 2009; Jung *et al.*, 2009; Rosenstiel *et al.*, 2009), it is likely that these key effector molecules of the innate immune system have an essential role in this regulation. Antimicrobial peptides in *Hydra* have been found to have different antimicrobial activities against different bacteria species (Bosch *et al.*, 2009; Jung *et al.*, 2009). It should therefore not be surprising if different antimicrobial peptides affect the microbiota associated with the hydra epithelium in a different manner.

Evidence presented in this study shows that the absence of two types of interstitial cell derivatives, nerve cells and secretory gland cells, has profound impact on the composition of the colonizing microbiota. Interestingly, both cell types have been observed earlier in being involved in *Hydra*'s microbial defence. When investigating the antibacterial activity in *Hydra*, we unexpectedly observed a strong correlation between the number of neurones present and the level of the antibacterial response (Kasahara and Bosch, 2003). Using the same mutant strain of *H. magnipapillata* containing temperature-sensitive interstitial stem cells as the strain used in this study, we observed strong antibacterial activity in epithelial tissue lacking any neurones suggesting that in *Hydra* neurones influence the innate immune response (Kasahara and Bosch, 2003). As it was probably within cnidarians, or a related ancestor group, that nervous systems first evolved (Nielsen, 2008), these observations led us to propose (Kasahara and Bosch, 2003) that the cross-talk between nervous and immune system should be considered as an evolutionary ancient invention. Our observation of drastic changes in the composition of the microbiota in polyps lacking nerve cells (Figs 2–4) underlines the significance of this cell type in host–microbe interactions.

Another cell type absent in temperature-treated *H. magnipapillata* strain sf1 polyps which is affecting the composition of the microbiota are secretory gland cells. Interestingly, our recent investigations show that *Hydra*'s secretory gland cells play important roles in preventing bacterial infection by producing antimicrobial mediators such as serin protease inhibitors belonging to the kazal type family (Augustin *et al.*, 2009). Together with the observations reported in the present study this suggests that the release of immune mediators from secretory gland cells may constitute a critical early step in the complex series of cellular and molecular events which make up the innate immune response in *Hydra*.

Although important first steps have been made in describing the microbiota of the *Hydra*, much needs to be

learned about their function. Which roles do microbial communities play in the health of *Hydra*? Does the microbial flora associated with *Hydra* contribute to the antimicrobial defence of the animal? What principles govern the assembly and maintenance of the hydra microbiome? Do antimicrobial peptides not only kill bacteria but are also involved in keeping the structure of the microbial community in balance? Answers to these questions will considerably improve our understanding of the role that tissue-associated microbial communities play in health and disease. As early as 1982, axenic *Hydra* were shown to have severe developmental defects (Rahat and Dimentman, 1982). Culturing them under sterile conditions resulted in reduced budding rate; after inoculation with bacteria from *Hydra* stock-culture normal budding was resumed. While there are several explanations for this effect, one attractive hypothesis could be that *Hydra* needs bacteria for normal tissue homeostasis.

In summary, our finding has three major implications. First, it indicates a previously unrecognized link between cellular tissue composition and microbiota. Second, the finding may be applicable to understanding mechanisms controlling host–microbe interaction in other epithelial systems. The complexity of most previously studied systems has limited detailed studies of epithelial influences on microbial distribution. Our findings derived from the *in vivo* context of a whole epithelial organism therefore may provide one of the simplest possible systems to address questions of how tissue composition affects the microbial community over space and time and how a stable host and microbe community remains in balance. Third, as *Hydra* is an early branching metazoan (Collins, 1998; Collins *et al.*, 2006) and has preserved much of the genetic complexity of the common metazoan ancestor (Miller *et al.*, 2007; Hemmrich and Bosch, 2008; Rosentiel *et al.*, 2009), it also promises to be highly informative with respect to tracing ancient mechanisms controlling inter–domain interaction between bacteria and their hosts.

Experimental procedures

Animal culture

Experiments were carried out with mutant strain *H. magnipapillata* sf1 containing a temperature-sensitive interstitial cell lineage (Sugiyama and Fujisawa, 1978). The ‘control_temp’ experiment was carried out with *H. magnipapillata* strain 105. Unless otherwise stated, animals were cultured using standard conditions at 18°C. Treatment of sf1 polyps, which have temperature-sensitive interstitial cells (Terada *et al.*, 1988), for 48 h at the restrictive temperature (28°C) induces quantitative loss of the entire interstitial cell lineage including interstitial stem cells, proliferating nematoblasts and differentiating nematocytes. Cell composition and cell number in polyps at various time points after temperature

treatment were determined in mazerated preparations (David, 1973). ‘Control starved’ animals represent *H. magnipapillata* strain sf1 polyps which were not exposed to temperature treatment but starved for up to 40 days. ‘Control temp’ animals represent *H. magnipapillata* strain 105 polyps which were exposed to temperature treatment in the same way as experimental animals and analysed for their bacterial composition 46 days after temperature treatment.

Molecular analysis

For genomic DNA extraction, whole animals were subjected to the DNeasy Tissue Kit (Qiagen, Hilden, Germany). Universal bacterial PCR primers were used to amplify the region corresponding to positions 27–1492 of the *Escherichia coli* 16S rRNA gene by using a 30 cycle PCR (Weisburg *et al.*, 1991). Resulting PCR fragments were cloned into pGEMT vector (Promega, Madison, Wisconsin) and transformed into *E. coli* DH5 α cells (Invitrogen, Karlsruhe, Germany). From each sample around 46 transformants were selected. Plasmid inserts were checked by PCR and subjected to RFLP by using the restriction enzymes HaeIII and Hin6I (Fermentas). By sequencing two to three clones with identical RFLP pattern, we confirmed that clones are members of the same phylotype. Representative plasmids were sequenced using a LI-COR 4300 DNA Analyzer plate sequencer (LICOR Biosciences, Lincoln, Nebraska). All sequences have been submitted to GenBank (FJ517665–FJ517723).

Data analysis

Sequences were sorted into phylotypes using the criterion of 99% sequence identity. All the sequences were subjected to the chimera check programs Bellerophon (Huber *et al.*, 2004) and Pintail (Ashelford *et al.*, 2005) for the elimination of chimeric sequences. Three sequences could be identified containing substantial anomalies and were removed from the data set. Chloroplast sequences were identified and removed. The final data set of 61 non-chimeric sequences were aligned using the ARB software package (Ludwig *et al.*, 2004). Closely related sequences were found by the function ‘search for the closest relatives’ implemented in the ARB software and by a BLAST search and added also to the alignment. Alignments were optimized by hand and a neighbour-joining tree was calculated with all 16S rDNA sequences and their closest relatives by using Olsen correction and a bootstrap resampling of 1000 replicates.

Quantitative real-time PCR

For two bacterial phylotypes showing drastic changes in their relative abundance due to the temperature treatment, phylotype-specific primers were designed using the computational tool Primrose 2.17 (Ashelford *et al.*, 2002). The primers used for quantitative RT-PCRs are summarized in Table 2. Quantitative RT-PCR assays were performed with a QuantiTect Probe RT-PCR Kit (Qiagen, Hilden, Germany) using a 7300 realtime PCR system (ABI, Foster City, USA). The amplification efficiency of each gene was tested with a dilution series from a reference gDNA. All amplification effi-

ciencies were comparable with a $\Delta C_{\text{slope}} < 0.1$. The fold change in abundance for 16S rRNA genes of interest was determined by comparison with the threshold cycle (C_t) of the control gene *Hydra* actin: hyActinF 5'-GAA TCA GCT GGT ATC CAT GAA AC-3' and hyActinR 5'-AAC ATT GTC GTA CCA CCT GAT AG-3'. The fold change in the abundance of 16S rRNA genes was calculated using the formula fold change = $2^{-\Delta\Delta C_t}$.

Data analysis with UniFrac

To test differences between the bacterial communities from each sample, we used the UniFrac computational tool (Lozupone and Knight, 2005). We used the neighbour-joining tree to calculate the fraction of tree branch length unique to any one treatment in pairwise comparisons (weighted UniFrac metric). The P -value for the tree, reflecting the probability that there are more unique branch lengths than expected by chance, was calculated by generating 1000 random trees. The analysis accounted for abundance information resulting from the RFLP analysis. Additionally we performed UPGMA clustering, using the weighted UniFrac metric and a jackknife analysis with 1000 permutations to access confidence in nodes of the UPGMA tree.

Estimation of diversity

The estimation of the number of bacterial phylotypes in each sample was assessed by the Chao1 non-parametric richness estimator implemented in the computational tool EstimateS (Version 8, <http://viceroy.eeb.uconn.edu/estimates>). For the purpose of inputting data into the program, we treated each RFLP pattern as a separate sample.

Acknowledgements

We thank René Augustin, Konstantin Khalturin, Philip Rosentiel and Ruth Schmitz-Streit for comments and Kristina Brandstädter for drawing the *Hydra* figures. Constructive comments from four anonymous reviewers are appreciated. Funding was provided in part by grants from the Deutsche Forschungsgemeinschaft (DFG, SFB 617-A1), and grants from the DFG Cluster of Excellence programs 'The Future Ocean' and 'Inflammation at Interfaces' (to T.C.G.B.).

References

Ashelford, K.E., Weightman, A.J., and Fry, J.C. (2002) PRIM-ROSE: a computer program for generating and estimating the phylogenetic range of 16S rRNA oligonucleotide probes and primers in conjunction with the RDP-II database. *Nucleic Acids Res* **30**: 3481–3489.

Ashelford, K.E., Chuzhanova, N.A., Fry, J.C., Jones, A.J., and Weightman, A.J. (2005) At least 1 in 20, 16S rRNA sequence records currently held in public repositories is estimated to contain substantial anomalies. *Appl Environ Microbiol* **71**: 7724–7736.

Augustin, R., Siebert, S., and Bosch, T.C.G. (2009) Identification of a kazal-type serine protease inhibitor with potent

anti-staphylococcal activity as part of hydra's innate immune system. *Dev Comp Immunol* **33**: 830–837.

Bosch, T.C. (2007) Symmetry breaking in stem cells of the basal metazoan Hydra. In *Asymmetric cell division Series: Progress in Molecular and Subcellular Biology*. Macieira-Coelho, A. (ed.). Heidelberg, Germany: Springer, pp. 61–78.

Bosch, T.C. (2008) Stem cells in immortal *Hydra*. In *Stem Cells: From Hydra to Man*. Bosch, T.C. (ed.). Heidelberg, Germany: Springer, pp. 37–57.

Bosch, T.C.G., Augustin, R., Anton-Erxleben, F., Fraune, S., Hemmrich, G., Zill, H., et al. (2009) Uncovering the evolutionary history of innate immunity: the simple metazoan Hydra uses epithelial cells for host defence. *Dev Comp Immunol* **33**: 559–569.

Cole, J.R., Chai, B., Farris, R.J., Wang, Q., Kulam-Syed-Mohideen, A.S., McGarrell, D.M., et al. (2007) The ribosomal database project (RDP-II): introducing *myRDP* space and quality controlled public data. *Nucleic Acids Res* **35** (Database issue): D169–D172. doi: 10.1093/nar/gkl889.

Collins, A.G. (1998) Evaluating multiple alternative hypotheses for the origin of Bilateria: an analysis of 18S rRNA molecular evidence. *Proc Natl Acad Sci USA* **95**: 15458–15463.

Collins, A.G., Schuchert, P., Marques, A.C., Jankowski, T., Medina, M., and Schierwater, B. (2006) Medusozoan phylogeny and character evolution clarified by new large and small subunit rDNA data and an assessment of the utility of phylogenetic mixture models. *Syst Biol* **55**: 97–115.

Dale, C., and Moran, N.A. (2006) Molecular interactions between bacterial symbionts and their hosts. *Cell* **126**: 453–465.

David, C.N. (1973) Quantitative method for maceration of hydra tissue. *Wilh Roux Arch Dev Biol* **171**: 259–263.

Frank, D.N., St Amand, A.L., Feldman, R.A., Boedeker, E.C., Harpaz, N., and Pace, N.R. (2007) Molecular-phylogenetic characterization of microbial community imbalances in human inflammatory bowel diseases. *Proc Natl Acad Sci USA* **104**: 13780–13785.

Fraune, S., and Bosch, T.C. (2007) Long-term maintenance of species-specific bacterial microbiota in the basal metazoan Hydra. *Proc Natl Acad Sci USA* **104**: 13146–13151.

Hemmrich, G., and Bosch, T.C. (2008) Compagen, a comparative genomics platform for early branching metazoan animals, reveals early origins of genes regulating stem-cell differentiation. *Bioessays* **30**: 1010–1018.

Hemmrich, G., Anokhin, B., Zacharias, H., and Bosch, T.C. (2007) Molecular phylogenetics in *Hydra*, a classical model in evolutionary developmental biology. *Mol Phylogenet Evol* **44**: 281–290.

Huber, T., Faulkner, G., and Hugenholtz, P. (2004) Bellerophon: a program to detect chimeric sequences in multiple sequence alignments. *Bioinformatics* **20**: 2317–2319.

Jung, S., Dingley, A.J., Augustin, R., Anton-Erxleben, F., Stanisak, M., Gelhaus, C., et al. (2009) Hydramacin-1: structure and antibacterial activity of a protein from the basal metazoan hydra. *J Biol Chem* **284**: 1896–1905.

Kasahara, S., and Bosch, T.C. (2003) Enhanced antibacterial

- activity in *Hydra* polyps lacking nerve cells. *Dev Comp Immunol* **27**: 79–85.
- Lozupone, C., and Knight, R. (2005) UniFrac: a new phylogenetic method for comparing microbial communities. *Appl Environ Microbiol* **71**: 8228–8235.
- Ludwig, W., Strunk, O., Westram, R., Richter, L., Meier, H., Yadhukumar, *et al.* (2004) ARB: a software environment for sequence data. *Nucleic Acids Res* **32**: 1363–1371.
- Mazmanian, S.K., Liu, C.H., Tzianabos, A.O., and Kasper, D.L. (2005) An immunomodulatory molecule of symbiotic bacteria directs maturation of the host immune system. *Cell* **122**: 107–118.
- Mazmanian, S.K., Round, J.L., and Kasper, D.L. (2008) A microbial symbiosis factor prevents intestinal inflammatory disease. *Nature* **453**: 620–625.
- Miller, D.J., Hemmrich, G., Ball, E.E., Hayward, D.C., Khalaturin, K., Funayama, N., *et al.* (2007) The innate immune repertoire in cnidaria – ancestral complexity and stochastic gene loss. *Genome Biol* **8**: R59.
- Muyzer, G., de Wall, E.C., and Uitterlinden, A.G. (1993) Profiling of complex microbial populations by denaturing gradient gel electrophoresis analysis of polymerase chain reaction-amplified genes coding for 16S rRNA. *Appl Environ Microbiol* **59**: 695–700.
- Nielsen, C. (2008) Six major steps in animal evolution: are we derived sponge larvae? *Evol Dev* **10**: 241–257.
- Ott, S.J., Musfeldt, M., Wenderoth, D.F., Hampe, J., Brant, O., Folsch, U.R., *et al.* (2004) Reduction in diversity of the colonic mucosa associated bacterial microflora in patients with active inflammatory bowel disease. *Gut* **53**: 685–693.
- Rahat, M., and Dimentman, C. (1982) Cultivation of bacteria-free *Hydra viridis*: missing budding factor in nonsymbiotic hydra. *Science* **216**: 67–68.
- Rakoff-Nahoum, S., Paglino, J., Eslami-Varzaneh, F., Edberg, S., and Medzhitov, R. (2004) Recognition of commensal microflora by toll-like receptors is required for intestinal homeostasis. *Cell* **118**: 229–241.
- Rosenstiel, P., Philipp, E., Schreiber, S., and Bosch, T.C.G. (2009) Evolution and function of innate immune receptors – insights from marine invertebrates. *J Innate Immunol* **1**: 291–300.
- Sugiyama, T., and Fujisawa, T. (1978) Genetic analysis of developmental mechanisms in *Hydra*. II. Isolation and characterization of an interstitial cell-deficient strain. *J Cell Sci* **29**: 35–52.
- Terada, H., Sugiyama, T., and Shigenaka, Y. (1988) Genetic analysis of developmental mechanisms in hydra. XVIII. Mechanism for elimination of the interstitial cell lineage in the mutant strain Sf-1. *Dev Biol* **126**: 263–269.
- Weisburg, W.G., Barns, S.M., Pelletier, D.A., and Lane, D.J. (1991) 16S ribosomal DNA amplification for phylogenetic study. *J Bacteriol* **173**: 697–703.

Supporting information

Additional Supporting Information may be found in the online version of this article:

Fig. S1. Sample-based assessments of diversity and coverage at different sampling time points after temperature treatment.

A and B. The number of observed phylotypes (99%ID) and the number of clones sampled are shown as Rarefaction curves.

C and D. The phylotype richness for each treatment is expressed as Chao1 richness estimates.

Please note: Wiley-Blackwell are not responsible for the content or functionality of any supporting materials supplied by the authors. Any queries (other than missing material) should be directed to the corresponding author for the article.